Original paper

Fatigue behavior and crack initiation of CAD/CAM resin composite molar crowns

Satoshi Yamaguchi[a*], Renshirou Kani[a], Kazuma Kawakami[a], Manami Tsuji[a], Sayuri Inoue[a,b], Chunwoo Lee[a], Wakako Kiba[a], Satoshi Imazato[a]

[a]Department of Biomaterials Science, Osaka University Graduate School of Dentistry, Osaka, Japan

[b]Department of Orthodontics and Dentofacial Orthopedics, Osaka University Graduate School of Dentistry, 1-8 Yamadaoka, Suita, Osaka 565-0871, Japan

*Correspondence should be addressed to Satoshi Yamaguchi

Department of Biomaterials Science, Osaka University Graduate School of Dentistry, 1-8 Yamadaoka, Suita, Osaka 565-0871, Japan

Tel/Fax: +81-6-6879-2917

E-mail: yamagu@dent.osaka-u.ac.jp

Declaration of interest statement

Funding

This research was supported by a Grant-in-Aid for Scientific Research (No. JP15K11195) from the Japan Society for the Promotion of Science (JSPS).

Abbreviations

CAD/CAM	computer-aided design/computer-aided manufacturing
SSALT	Step-stress accelerated life test
FEA	Finite element analysis
MPS	Maximum principal strain
RCB	Resin composite block
PVC	Polyvinyl chloride
XRD	X-ray diffraction
SEM	Scanning electron microscopy
ANOVA	Analysis of variance
HSD	honest significant difference

ABSTRACT

Objective: The aim of this study was to evaluate long-term fatigue behavior using an *in vitro* step-stress accelerated life test (SSALT), and to determine the crack initiation point using *in silico* finite element analysis for computer-aided designed and manufactured (CAD/CAM) molar crowns fabricated from three commercial CAD/CAM resin composite blocks: Cerasmart (CS; GC, Tokyo, Japan), Katana Avencia Block (KA; Kuraray Noritake Dental, Niigata, Japan), and Shofu Block HC (HC; Shofu, Kyoto, Japan).

Methods: Fifty-one mandibular first molar crowns luted on a resin core die were embedded in acrylic resin and covered with a polyvinyl chloride tube. Single compressive tests were performed for five crowns. SSALT was conducted for 36 crowns using three profiles and reliabilities at 120,000 cycles, and a Weibull analysis was conducted. The maximum principal strain of each CAD/CAM resin composite crown model was analyzed by three-dimensional finite element analysis.

Results: Fracture loads of CS and KA (3784 ± 144 N and 3915 ± 313 N) were significantly greater than that of HC (2767 ± 227 N) ($p < 0.05$). Fracture probabilities at 120,000 cycles were 24.6% (CS), 13.7% (KA), and 14.0% (HC). Maximum principal strain was observed around the mesiolingual cusps of CS and KA and the distobuccal cusp of HC.

Significance: CAD/CAM resin composite molar crowns containing nano-fillers with a higher fraction of resin matrix exhibited higher fracture loads and greater longevity, suggesting that these crowns could be used as an alternative to ceramic crowns in terms of fatigue behavior.

KEYWORDS

CAD/CAM resin composite molar crown, CAD/CAM resin composite, fatigue resistance, step-stress accelerated life testing, three-dimensional finite element analysis

1 INTRODUCTION

Computer-aided design / computer-aided manufacturing (CAD/CAM) resin composite blocks (RCBs) containing a high density of nano-filler particles are available for use in posterior restorations [1]. Because of the preliminary polymerized resin matrix, the nano-filler particles are homogeneously dispersed in the resin matrix, providing stable and excellent mechanical properties such as flexural strength and fracture toughness when compared with those of conventional resin composites used in fillings [2, 3]. As an alternative material to metals or ceramics, CAD/CAM RCBs are attracting much attention because their esthetics are more favorable than metals and their cost is lower than ceramics [4]. CAD/CAM RCBs have excellent fatigue resistance with no catastrophic failures when compared with ceramics [5]. The resin matrix of CAD/CAM RCBs prevents crack propagation during cyclic loading and leads to greater flexural strength and a lower flexural modulus [6].

The long-term fatigue behavior of bar-shaped CAD/CAM RCB specimens after fatigue treatment has been measured using a three-point bending test, and was found to be comparable to lithium disilicate glass-ceramic [7]. However, the fatigue behavior of crown-shaped specimens is still unknown. A frequency of 15 Hz with a load of 10–40 N for 1.2×10^6 cycles (~22 hours) is required to prepare each specimen for the three-point bending test.

A step-stress accelerated life test (SSALT) that mimics the sliding contact movement in the mouth has been used to investigate the longevity of dental implants [8] and all-ceramic crowns [9, 10]. Fracture patterns of bar-shaped specimens after fatigue tests with or without step-stress profiles were similar; that is, SSALT has been validated and could be more time-efficient than fatigue testing with a constant load [11]. The fatigue behavior of CAD/CAM resin composite crowns has been evaluated and was found to be comparable to leucite reinforced glass-ceramic crowns, with no catastrophic failures occurring in the CAD/CAM resin composite crowns [5]. The fracture pattern of crown-shaped specimens after catastrophic failure is important to ascertain the crack initiation point and to improve the composition and physical properties of CAD/CAM resin composite. Fractographic analysis has been used to evaluate the fractured surface after SSALT for dental implants [12, 13], ceramics [14], and polymer infiltrated ceramic network materials [15]. However, it is difficult to determine the specific crack initiation point because the fracture has already occurred.

Finite element analysis (FEA) is a powerful tool for calculating stress and strain distribution in dental implants [16, 17] and CAD/CAM RCBs [18]. FEA can be used to predict the crack initiation point by using maximum principal strain as an effective failure criteria [19].

The aim of this study was to evaluate long-term fatigue behavior using *in vitro* SSALT, and to determine the crack initiation point using *in silico* FEA for CAD/CAM resin composite molar crowns fabricated from three commercial CAD/CAM RCBs: Cerasmart (CS; GC, Tokyo, Japan), Katana Avencia Block (KA; Kuraray Noritake Dental, Niigata, Japan), and Shofu Block HC (HC; Shofu, Kyoto, Japan).

2 MATERIALS AND METHODS

2.1. CAD/CAM RCBs

Three types of commercially available CAD/CAM RCBs were used: Cerasmart (CS; GC, Tokyo, Japan), Katana Avencia Block (KA; Kuraray Noritake Dental, Niigata, Japan), and Shofu Block HC (HC; Shofu, Kyoto, Japan). Details of the composition of each block is shown in Table 1.

2.2. Specimen preparation

An impression was taken of a mandibular first molar abutment tooth model (A55A-461, Nissin, Kyoto, Japan) using silicone impression material. A total of 51 abutment teeth were fabricated by incremental build-up and photopolymerization of core resin (Clearfil DC Core Automix, Kuraray Noritake Dental) in the impression cavity. The mandibular right first molar model (A5A-500, Nissin) and the abutment tooth were scanned (SC-5, Kuraray Noritake Dental) and designed (DentalDesigner, Kuraray Noritake Dental). Both models were fabricated using a milling machine (DWX-50, Kuraray Noritake Dental). To strengthen the adhesion of the crowns [20], the inner surface of the crowns were sand blasted with an air pressure of 0.2 MPa using Al_2O_3 particles 30–50 μm in diameter. After ultrasonic cleaning for 2 minutes and air-drying, the inner surface of the crowns was etched with phosphoric acid gel (K-etchant gel, Kuraray Noritake Dental). After 5 seconds, ceramic primer (Clearfil Ceramic Primer, Kuraray Noritake Dental) was applied after rinsing with water and air-drying. The crowns were cemented on the abutment tooth and exposed to light for 5 seconds, followed by removal of excess cement.

2.3. Single compressive testing

All specimens were vertically embedded in a 25-mm diameter polyvinyl chloride (PVC) tube of acrylic resin (Unifast Lab type F, GC, Tokyo, Japan) with the buccal margin of the crown positioned 2 mm higher than the top surface of the acrylic resin. After storage in distilled water at 37 °C for 24 hours, a single compressive test (AGS-500D, Shimadzu, Kyoto, Japan) was performed at a crosshead speed of 0.5 mm/min ($n = 5$), and mean fracture load and standard deviation were calculated.

2.4. Step-stress accelerating life testing

Based on the mean load of the static compression test, three fatigue loading profiles were designed for the 12 specimens for SSALT [8]. The designed profiles were designated as mild ($n = 6$), moderate ($n = 4$), and aggressive ($n = 2$), following the ratio of 3:2:1 (**Fig. 1**). The crowns were immersed in distilled water (**Fig. 2**) during SSALT. SSALT was performed at a frequency of 5 Hz. Weibull analysis and a reliability assessment were conducted. Fractured specimens were observed with stereomicroscopy (SMZ-745T, Nikon, Tokyo, Japan) using high dynamic range software (NIS-Elements Ver.4.0, Nikon) and scanning electron microscopy (SEM; JSM-6390BU, JEOL, Tokyo, Japan) with 20× magnification at 5 kV.

2.5. Three-dimensional finite element analysis

FEA models of the indenter, crown, cement, die, acrylic resin, and PVC tube were designed from scanned stereolithography data (**Fig. 3**) for *in vitro* tests and analyzed using voxel-based FEA software (VOXELCON2015, Quint, Tokyo, Japan). Fracture loads after single compression tests were applied to the crown, and the location of the maximum principal strain on the crown was analyzed.

2.6. Statistical analysis

Mean fracture loads obtained from the single compression tests were analyzed by analysis of variance (ANOVA) and Tukey's honest significant difference (HSD) test (PASW Statistics 18, IBM, Somers, NY, USA). *P*-values of less than 0.05 were considered as statistically significant.

3. RESULTS

3.1. Fracture loads after single compression test

Fracture loads of CS (3784 ± 144 N) and KA (3915 ± 313 N) were significantly higher than that of HC (2767 ± 227 N) ($p < 0.05$) as shown in Figure 4. An initial load of three profiles for SSALT was determined from ~6% of the mean fracture load of 3489 N (i.e. 200 N).

3.2. Fracture reliability after SSALT

Weibull curves obtained from SSALT are presented in Figure 5. The shape parameter m (two-sided at 90% confidence bounds) for CS, KA, and HC were 3.8 (1.6–5.5), 3.1 (1.3–4.4), and 4.8 (2.0–6.9), respectively; and the scale parameter η (two-sided at 90% confidence bounds) for CS, KA, and HC were 2844.1 (2227.8–3695.7), 3672.0 (2706.5–5093.1), and 2774.8 (2279.6–3426.1), respectively. Greater reliability at 2000 N, 2500 N, and 3000 N was recorded for KA (85.7%, 73.6%, and 58.5%) than HC (81.1%, 54.5%, and 23.4%) and CS (77.2%, 54.4%, and 29.3%). Fracture probabilities at 120,000 cycles were 24.6% (CS), 13.7% (KA), and 14.0% (HC).

3.3. Fractographic analysis

Figure 6 shows stereoscopic images from the occlusal surface after SSALT with an aggressive profile for CS, KA, and HC. Most of the specimens fractured along the central sulcus of each crown. Figure 7 shows SEM images from the lingual side after SSALT with an aggressive profile for CS, KA, and HC. Large white arrows indicate crack initiation points. Arrested lines indicated by small white arrows were observed throughout the fracture surface of the crowns. Hackle patterns following the direction of crack propagation are indicated by asterisks.

3.4. Maximum principal strain (MPS)

The MPS was observed around the mesiolingual cusp for CS (**Fig. 8a**) and KA (**Fig. 8b**), and around the distobuccal cusp for HC (**Fig. 8c**). Large white arrows indicate the location of the MPS.

DISCUSSION

CAD/CAM resin composite crowns fabricated from CAD/CAM RCBs have been used as restorations to replace lost tooth structure. After approval by Japanese health insurance companies in 2014, the restoration of premolars and molars with CAD/CAM resin composite crowns has grown as an alternative to metal and ceramic restorations. In this study, the long-term fatigue behavior of three commercial CAD/CAM resin composite molar crowns was elucidated *in vitro* and the crack initiation points at the crowns were determined *in silico*.

The X-ray diffraction (XRD) patterns of all CAD/CAM resin composite powders showed a typical amorphous phase and an increasing order of broad peaks that have been reported by Yoshihara *et al*. [21]. The broad peak of 22.0º [22] for KA and HC were derived from SiO_2 particles, and the other peak of 26.5º [23] for CS was derived from BaO fillers. HC contained spherical filler particles ranging between 1.0 and 10.0 µm [21], which is one of the reasons it exhibited a higher peak in the XRD patterns than the other two CAD/CAM resin composites.

CS and KA contained nano-fillers of 20-nm and 40-nm SiO_2 particles, respectively, and exhibited higher fracture loads after the single compressive test. We have clarified that the compressive strength of CAD/CAM RCBs can be enhanced by loading with silica nano-filler particles of smaller diameter [18]. Fracture loads after the single compressive test using crown-shaped specimens were also consistent with our previous findings.

In the Weibull analysis, the lower shape parameter m of KA indicated greater reliability in strength when compared with CS and HC. Additionally, the higher scale parameter η for KA indicated that the load in 63.2% of specimens that failed was higher than those of CS and HC. Interestingly, the order of increase in fracture load after single compressive tests (HC < CS < KA) did not match the order of increase in reliability after SSALT (CS < HC < KA). The filler fractions of KA and HC were 62 wt% and 61 wt%, while that of CS was 71 wt%; thus, the resin matrix fraction of KA and HC should be higher than that of CS. Therefore, the resin matrix of KA and HC could prevent crack propagation during SSALT and might show greater fatigue behavior than CS. The higher fraction of resin matrix might increase the bonding ability between the inner surface of CAD/CAM resin composite crowns and the luting cement, while presenting a risk of an increased amount of water absorption affected by the structure of the polymers. Compared with the leucite reinforced glass ceramics (IPS Empress CAD) used by Shembish *et al*. [5], all the CAD/CAM resin composite crowns used in this study recorded a higher fracture load and greater reliability. The reliability of the IPS

Empress CAD molar crowns used in Shembish *et al.*'s study was 90% at 1,250,000 cycles and a clinically relevant load of 200 N, which simulates ~5 years of *in vivo* wear [5]. Sandblasting before bonding could roughen the surface and increase the surface area for bonding [20, 24]. The results of the fatigue behavior suggest that all the CAD/CAM composite crowns in our study have the potential to last more than 5 years in a clinical situation.

The total time of SSALT using three profiles at 5 Hz was 852,000 s (~10 days) for 12 crown-shaped specimens, while normal fatigue tests use 1,250,000 cycles at 2 Hz for 7,500,000 s (~87 days), indicating that SSALT could save 8.8 times as much time as normal fatigue tests.

MPS is applicable as a failure criterion and is effective in predicting the flexural strength of composite resins [19]. The crack initiation point of HC was different from other CAD/CAM resin composite molar crowns because of the significantly lower fracture load of HC compared with those of KA and CS. By increasing the load on HC for the FEA, the crack initiation point of HC must migrate from the distal cusp to the mesiolingual cusp as in KA and CS. As shown in Figure 8a, the crack initiation point was observed around the distal cusp, but the catastrophic failure occurred around the mesiolingual cusp. By fractographic analysis, two crack initiation points for all the

CAD/CAM resin composite molar crowns were considered as candidates in the SEM images. The FEA results could help to determine that the actual crack initiation occurred around the mesiolingual cusp. The crack initiation point was similar to that of zirconia-supported all-ceramic crowns [25].

The investigation of the pure resin matrix is ongoing to clarify how water absorption alters the mechanical properties of bulk CAD/CAM RCBs. An *in silico* nano-scale model of CAD/CAM RCBs [18] investigating the effect of silane coupling is under development to evaluate the influence of hydrolysis on the mechanical properties [26]. Further studies will accelerate improvements in the long-term fatigue behavior of CAD/CAM resin composite molar crowns.

CONCLUSIONS

CAD/CAM resin composite molar crowns containing nano-fillers with a higher fraction of resin matrix demonstrated higher fracture loads and greater longevity, suggesting that these crowns could be used as an alternative to ceramic crowns in terms of fatigue behavior.

ACKNOWLEDGEMENTS

This research was supported by a Grant-in-Aid for Scientific Research (No. JP15K11195) from the Japan Society for the Promotion of Science (JSPS).

We thank Helen Jeays, BDSc AE, from Edanz Group (www.edanzediting.com/ac) for editing a draft of this manuscript.

REFERENCES

[1] Ruse ND, Sadoun MJ. Resin-composite blocks for dental CAD/CAM applications. J Dent Res, 2014; 93: 1232-4.

[2] Nguyen JF, Migonney V, Ruse ND, Sadoun M. Resin composite blocks via high-pressure high-temperature polymerization. Dent Mater, 2012; 28: 529-34.

[3] Giordano R. Materials for chairside CAD/CAM-produced restorations. J Am Dent Assoc, 2006; 137 Suppl: 14S-21S.

[4] Nguyen JF, Migonney V, Ruse ND, Sadoun M. Properties of experimental urethane dimethacrylate-based dental resin composite blocks obtained via thermo-polymerization under high pressure. Dent Mater, 2013; 29: 535-41.

[5] Shembish FA, Tong H, Kaizer M, Janal MN, Thompson VP, Opdam NJ, Zhang Y. Fatigue resistance of CAD/CAM resin composite molar crowns. Dent Mater, 2016; 32: 499-509.

[6] Lawson NC, Bansal R, Burgess JO. Wear, strength, modulus and hardness of CAD/CAM restorative materials. Dent Mater, 2016; 32: e275-e83.

[7] Ankyu S, Nakamura K, Harada A, Hong G, Kanno T, Niwano Y, Ortengren U, Egusa H. Fatigue analysis of computer-aided design/computer-aided manufacturing resin-based composite vs. lithium disilicate glass-ceramic. Eur J Oral Sci, 2016; 124:

387-95.

[8] Yamaguchi S, Yamanishi Y, Machado LS, Matsumoto S, Tovar N, Coelho PG, Thompson VP, Imazato S. In vitro fatigue tests and in silico finite element analysis of dental implants with different fixture/abutment joint types using computer-aided design models. J Prosthodont Res, 2018; 62: 24-30.

[9] Coelho PG, Bonfante EA, Silva NR, Rekow ED, Thompson VP. Laboratory simulation of Y-TZP all-ceramic crown clinical failures. J Dent Res, 2009; 88: 382-6.

[10] Rekow D, Thompson VP. Engineering long term clinical success of advanced ceramic prostheses. J Mater Sci Mater Med, 2007; 18: 47-56.

[11] Borba M, Cesar PF, Griggs JA, Della Bona A. Step-stress analysis for predicting dental ceramic reliability. Dent Mater, 2013; 29: 913-8.

[12] Bordin D, Bergamo ETP, Bonfante EA, Fardin VP, Coelho PG. Influence of platform diameter in the reliability and failure mode of extra-short dental implants. J Mech Behav Biomed Mater, 2018; 77: 470-4.

[13] Bordin D, Bergamo ETP, Fardin VP, Coelho PG, Bonfante EA. Fracture strength and probability of survival of narrow and extra-narrow dental implants after fatigue testing: In vitro and in silico analysis. J Mech Behav Biomed Mater, 2017; 71: 244-9.

[14] Baldassarri M, Zhang Y, Thompson VP, Rekow ED, Stappert CF. Reliability and

failure modes of implant-supported zirconium-oxide fixed dental prostheses related to veneering techniques. J Dent, 2011; 39: 489-98.

[15] El Zhawi H, Kaizer MR, Chughtai A, Moraes RR, Zhang Y. Polymer infiltrated ceramic network structures for resistance to fatigue fracture and wear. Dent Mater, 2016; 32: 1352-61.

[16] Yamanishi Y, Yamaguchi S, Imazato S, Nakano T, Yatani H. Effects of the implant design on peri-implant bone stress and abutment micromovement: three-dimensional finite element analysis of original computer-aided design models. J Periodontol, 2014; 85: e333-8.

[17] Yamanishi Y, Yamaguchi S, Imazato S, Nakano T, Yatani H. Influences of implant neck design and implant-abutment joint type on peri-implant bone stress and abutment micromovement: three-dimensional finite element analysis. Dent Mater, 2012; 28: 1126-33.

[18] Yamaguchi S, Inoue S, Sakai T, Abe T, Kitagawa H, Imazato S. Multi-scale analysis of the effect of nano-filler particle diameter on the physical properties of CAD/CAM composite resin blocks. Comput Methods Biomech Biomed Engin, 2017; 20: 714-9.

[19] Yamaguchi S, Mehdawi IM, Sakai T, Abe T, Inoue S, Imazato S. In vitro/in silico investigation of failure criteria to predict flexural strength of composite resins. Dent

Mater J, 2018; 37: 152-6.
[20] Higashi M, Matsumoto M, Kawaguchi A, Miura J, Minamino T, Kabetani T, Takeshige F, Mine A, Yatani H. Bonding effectiveness of self-adhesive and conventional-type adhesive resin cements to CAD/CAM resin blocks. Part 1: Effects of sandblasting and silanization. Dent Mater J, 2016; 35: 21-8.
[21] Yoshihara K, Nagaoka N, Maruo Y, Nishigawa G, Irie M, Yoshida Y, Van Meerbeek B. Sandblasting may damage the surface of composite CAD-CAM blocks. Dent Mater, 2017; 33: e124-e35.
[22] Bhattacharjee B, Ganguli D, Chaudhuri S, Pal AK. Synthesis and optical characterization of sol-gel derived zinc sulphide nanoparticles confined in amorphous silica thin films. Mater Chem Phys, 2003; 78: 372-9.
[23] Al-Hajry A, Al-Shahrani A, El-Desoky MM. Structural and other physical properties of barium vanadate glasses. Mater Chem Phys, 2005; 95: 300-6.
[24] Kawaguchi-Uemura A, Mine A, Matsumoto M, Tajiri Y, Higashi M, Kabetani T, Hagino R, Imai D, Minamino T, Miura J, Yatani H. Adhesion procedure for CAD/CAM resin crown bonding: Reduction of bond strengths due to artificial saliva contamination. J Prosthodont Res, 2017.
[25] Bonfante EA, Sailer I, Silva NR, Thompson VP, Dianne Rekow E, Coelho PG.

Failure modes of Y-TZP crowns at different cusp inclines. J Dent, 2010; 38: 707-12.

[26] Sideridou I, Tserki V, Papanastasiou G. Study of water sorption, solubility and modulus of elasticity of light-cured dimethacrylate-based dental resins. Biomaterials, 2003; 24: 655-65.

TABLES

Table 1. Composition of the CAD/CAM resin composite blocks.

Trade name	Code	Manufacturer	Composition		
			Monomer	Filler	Filler (wt%)
Cerasmart	CS	GC, Tokyo, Japan	Bis-MEPP, UDMA, DMA	SiO_2 (20 nm), Ba glass (300 nm)	71
Katana Avencia Block	KA	Kuraray Noritake Dental, Niigata, Japan	UDMA	SiO_2 (40 nm), Al_2O_3 (20 nm)	62
Shofu Block HC	HC	Shofu, Kyoto, Japan	UDMA, TEGDMA	SiO_2, microfumed SiO_2, zirconium silicate	61

Table 2. Properties of the CAD/CAM resin composite crowns used for finite element analysis.

	Crown			Indenter	Cement	PVC tube	Die and resin
Material	CS	KA	HC	Stainless steel	Panavia	Polyvinyl chloride	Acrylic resin
Elastic modulus (GPa)	8.4	8.5	12.2	210	12	1.5	2.979
Poisson's ratio	0.3	0.34	0.3	0.3	0.33	0.35	0.4

FIGURE LEGENDS

Figure 1. SSALT profiles showing the cycle-to-load assignment for specimens undergoing mild, moderate, or aggressive fatigue profiles.

Figure 2. Experimental setup of *in vitro* SSALT. The assembled CAD/CAM resin composite crown embedded in acrylic resin and covered with PVC tube was set onto a custom-made jig. Specimens were stored in water during SSALT.

Figure 3. CAD models of the indenter, crown, cement, die, acrylic resin, and PVC tube for three-dimensional finite element analysis.

Figure 4. Mean fracture loads after single compressive testing. Error bar indicates standard deviations. Asterisks indicate significant differences by one-way ANOVA and Tukey's honest significant difference test ($p < 0.05$).

Figure 5. Weibull curves from SSALT using CAD/CAM resin composite crowns for HC, CS, and KA.

Figure 6. Stereomicroscopic images processed using high dynamic range software after SSALT with an aggressive profile. (a) HC, (b) CS, and (c) KA.

Figure 7. SEM images of the fractured surface after SSALT with an aggressive profile for (a) HC, (b) CS, and (c) KA. Large white arrows indicate crack initiation points. Arrested lines are indicated by small white arrows. Hackle patterns following the direction of crack propagation are indicated by asterisks.

Figure 8. Maximum principal strain distribution at the crown of (a) HC, (b) CS, and (c) KA.

Figure 1

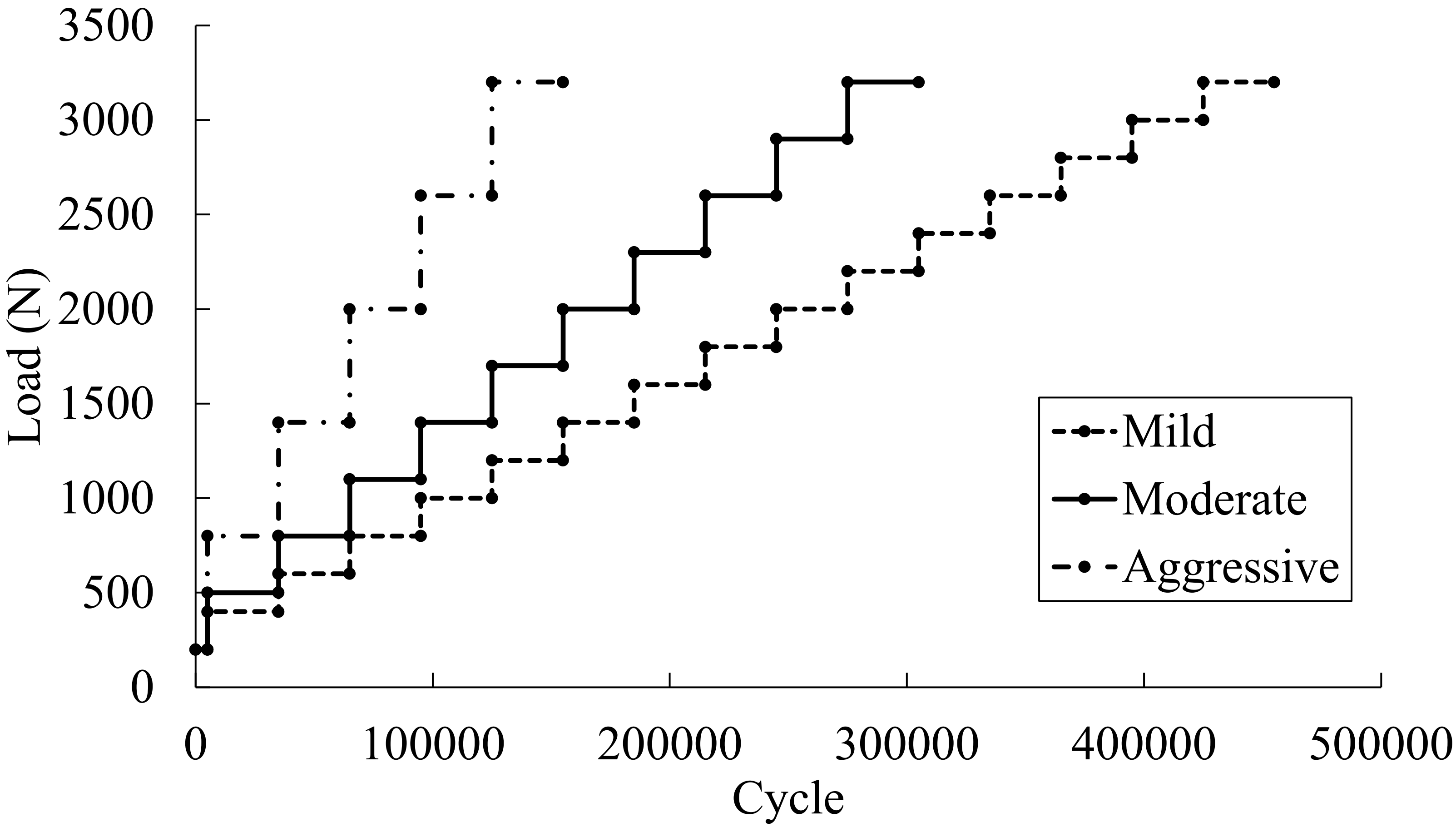

3500
3000
2500
2000
1500
1000
500
0
Load (N)
0
100000
200000
300000
400000
500000
Cycle
Mild
Moderate
Aggressive

Figure 2

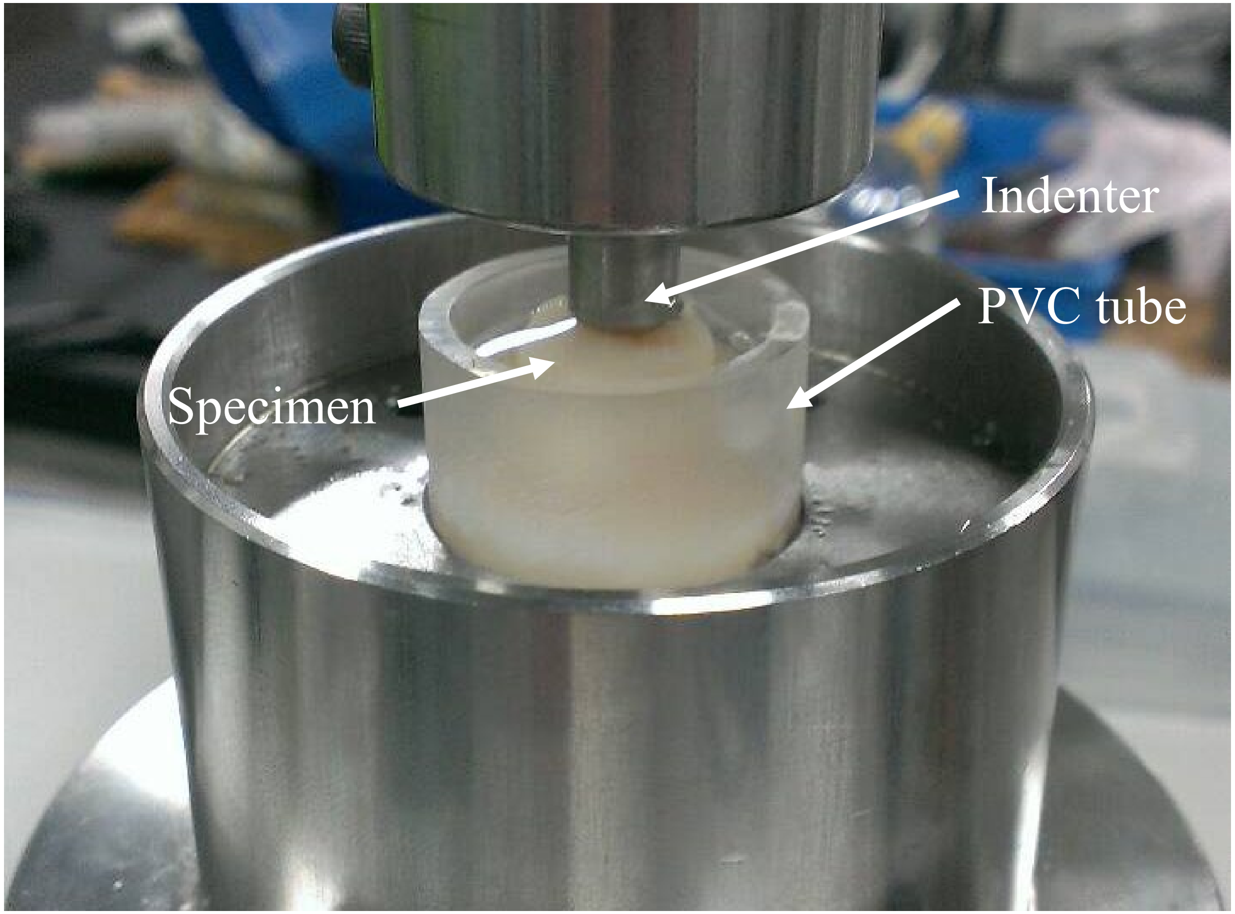

Figure 3

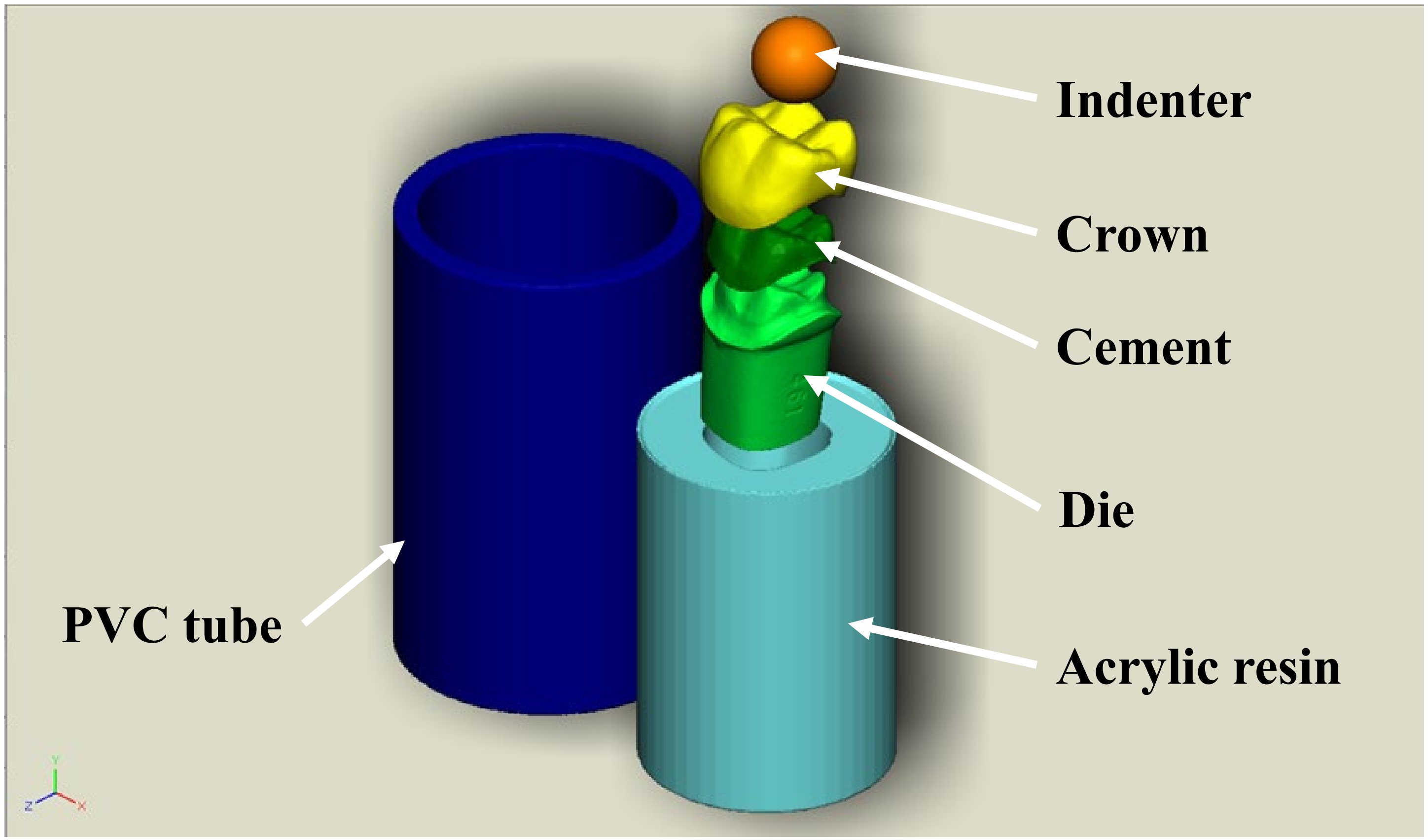

Figure 4

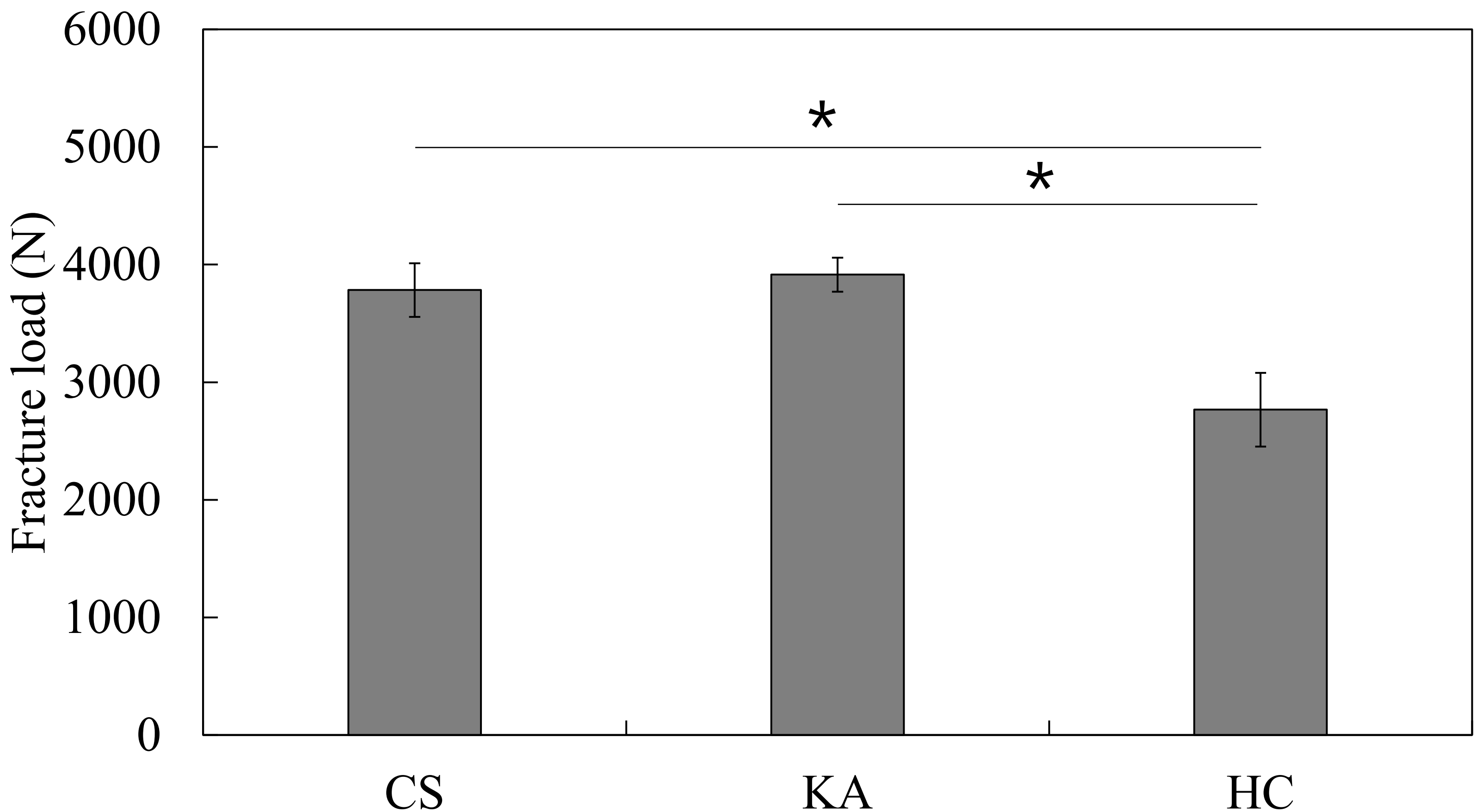

One-way ANOVA, Tukey's HSD test (**p*** **< 0.05)**

Figure 5

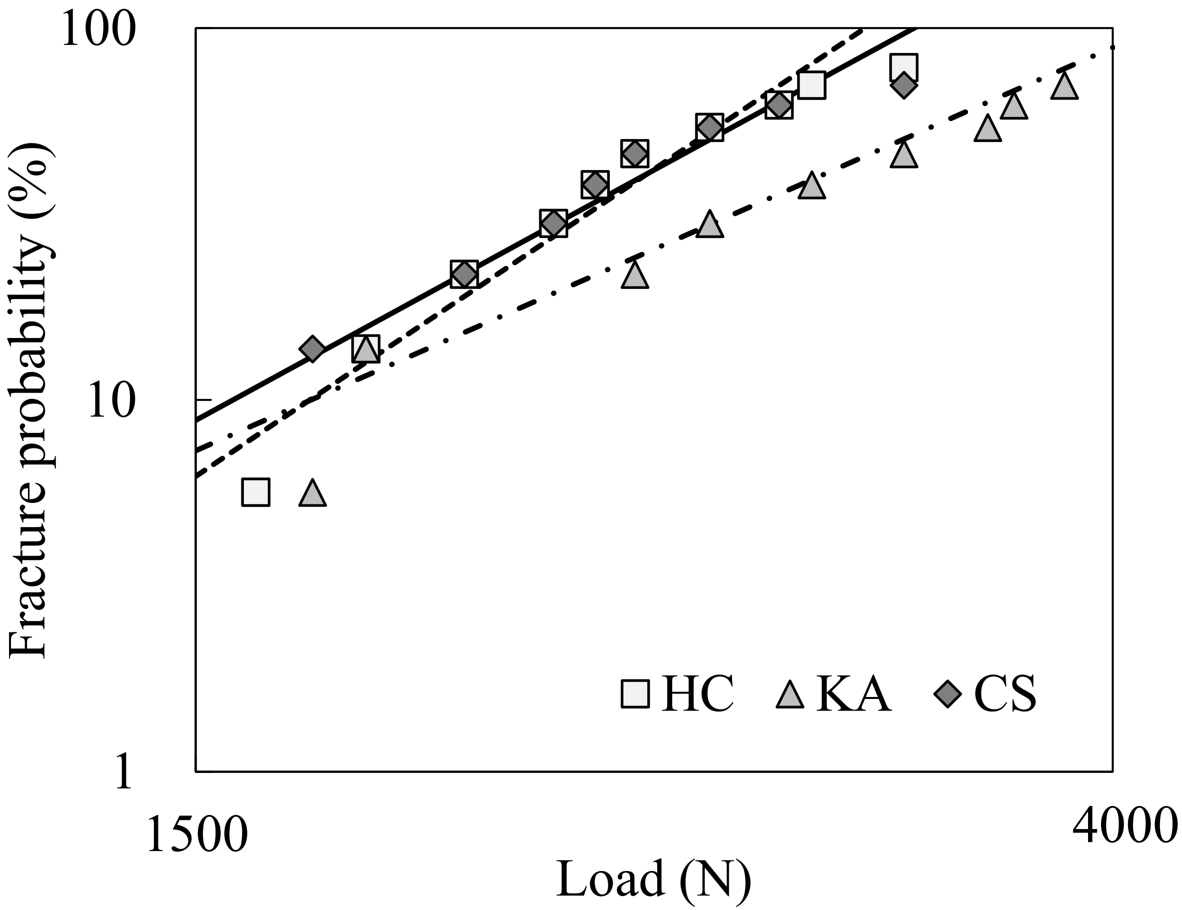

Figure 6

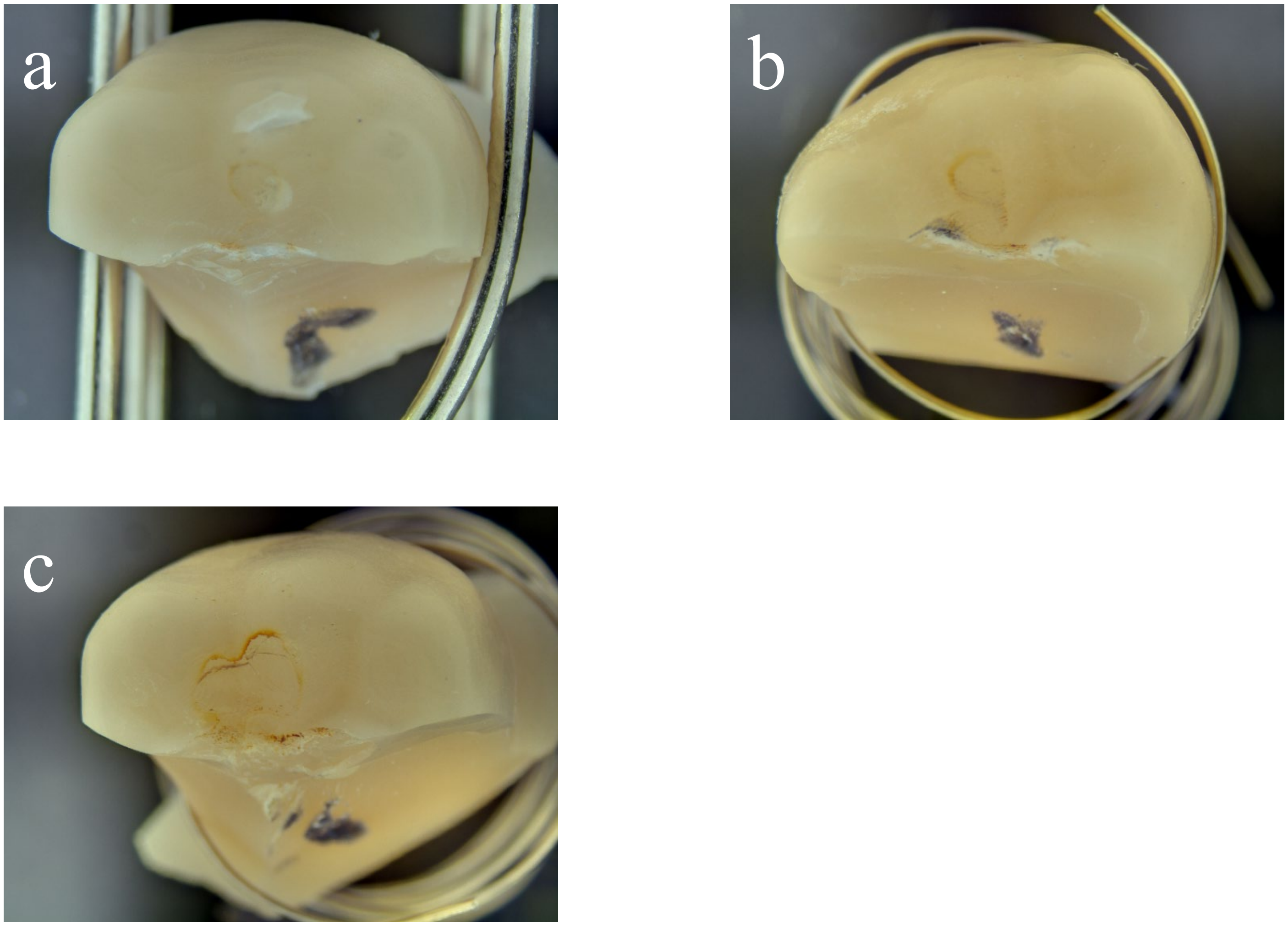

Figure 7

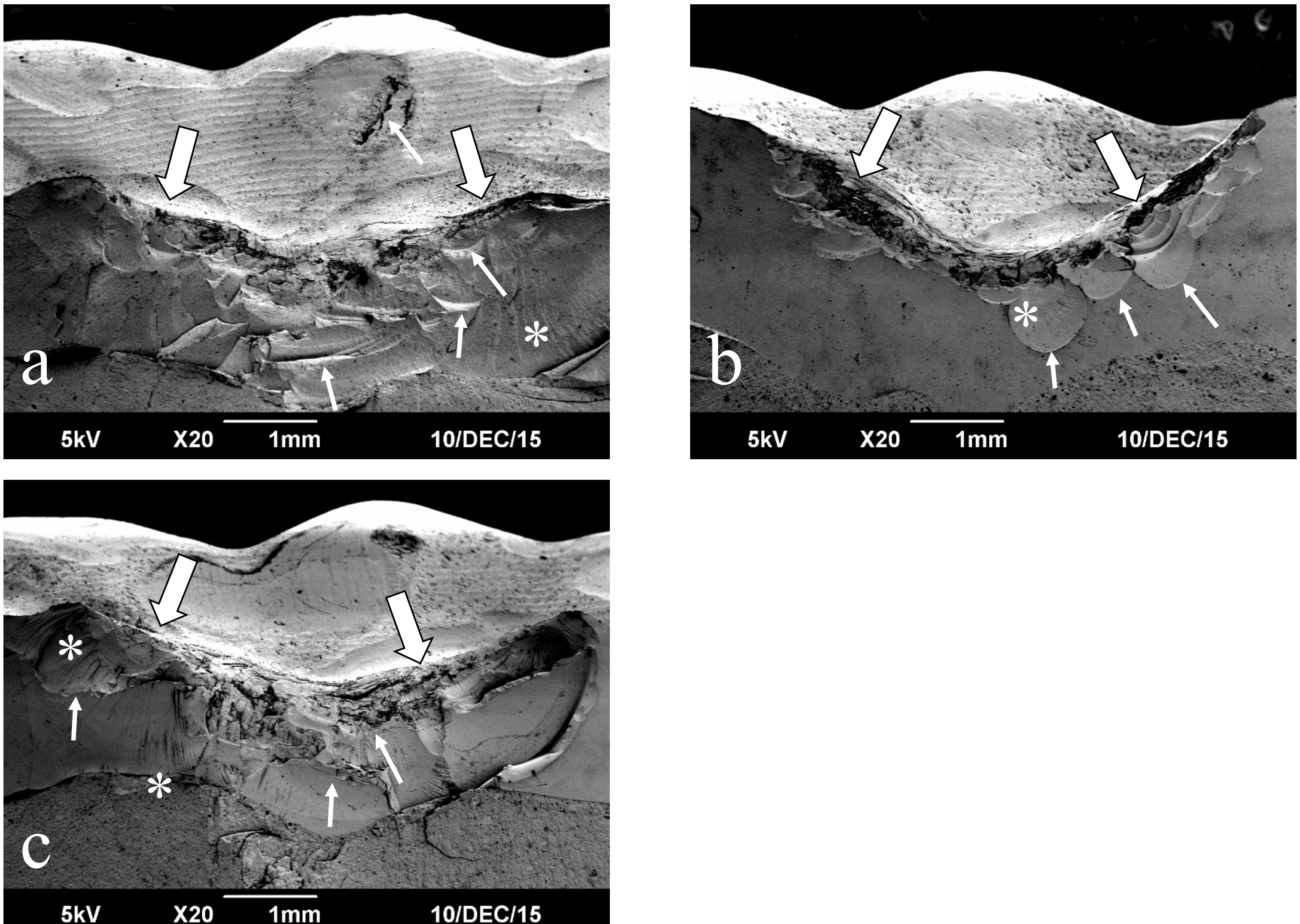
a
5kV X20 1mm 10/DEC/15
b
5kV X20 1mm 10/DEC/15
c
5kV X20 1mm 10/DEC/15

Figure 8

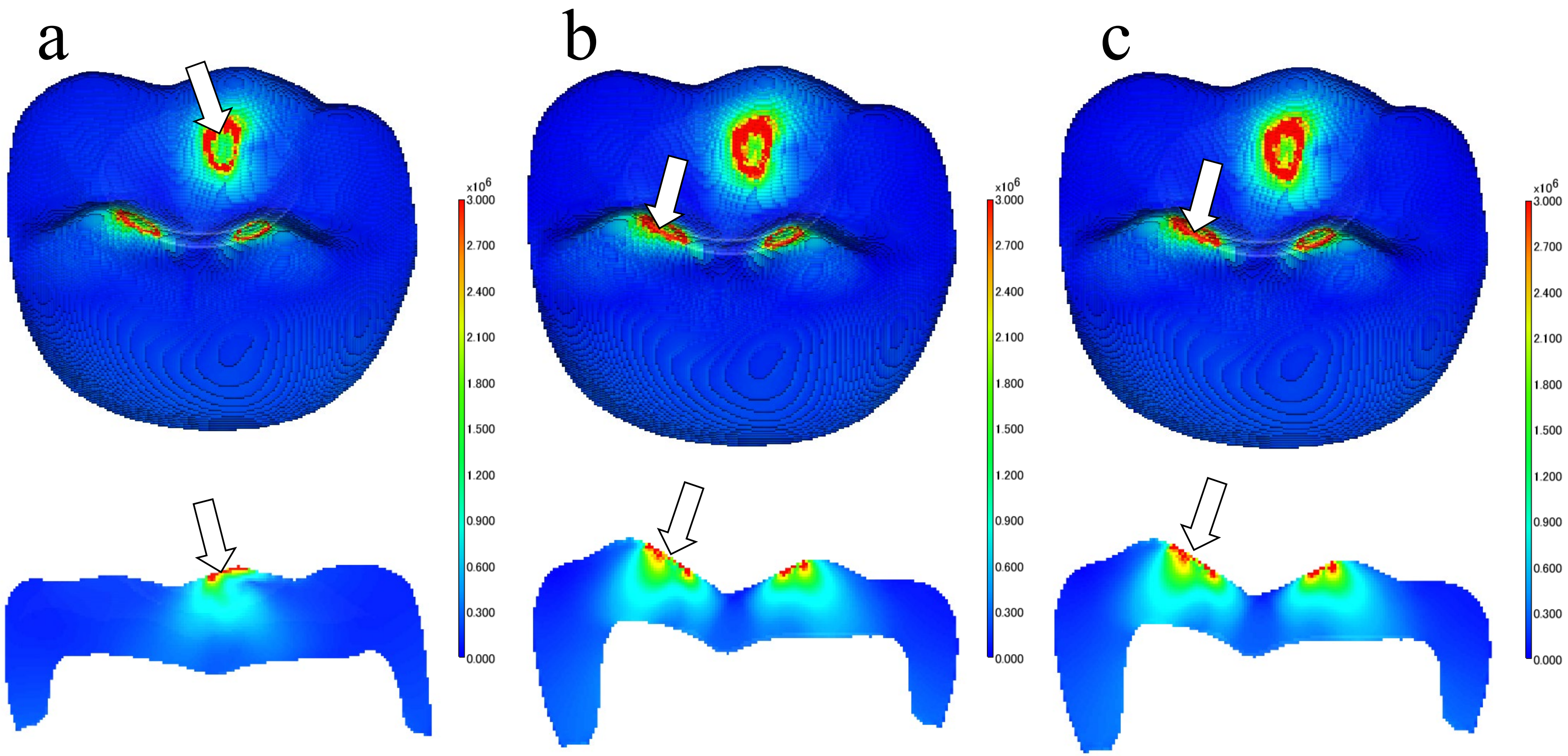
a
b
c
x10^6
3.000
2.700
2.400
2.100
1.800
1.500
1.200
0.900
0.600
0.300
0.000